



Magneto-Hydrodynamic Flow in a Two-Dimensional Inclined Rectangular Enclosure Heated and Cooled on Adjacent Walls

N. M. Kherief^{1†}, F. Berrahil² and K. Talbi²

¹*Normal High School of Technology Education ENSET-azzaba Skikda (Algeria).*

²*Department of Mechanical Engineering Mentouri University Constantine(Algeria).*

†Corresponding Author Email: kherief2006@yahoo.fr

(Received September 8, 2014; accepted December 19, 2014)

ABSTRACT

Steady, laminar, natural-convection flow in the presence of a magnetic field in an inclined rectangular enclosure heated from one side and cooled from the adjacent side was considered. The governing equations were solved numerically for the stream function, vorticity and temperature using the finite-volume method for various Grashof and Hartman numbers and inclination angles and magnetic field directions. The results show that the orientation and the strength and direction of the magnetic field have significant effects on the flow and temperature fields. Counterclockwise inclination induces the formation of multiple eddies inside the enclosure significantly affecting the temperature field. Circulation inside the enclosure and therefore the convection become stronger as the Grashof number increases while the magnetic field suppresses the convective flow and the heat transfer rate.

Keywords: Natural convection; Magnetic field; Inclined rectangular enclosure finite-volume; Lorentz force.

NOMENCLATURE

A	aspect ratio	Ra	Rayleigh number ($= \frac{g\beta(T_H - T_C)H^3}{\alpha\nu}$)
B	magnetic field [T]	R_m	Reynolds magnetic number
b	term source	S_ϕ	term source
e_B	unitary vector of the direction of B	T	temperature, [K]
F_x	lorentz force in the x-direction	T_C	cold temperature [K]
F_y	lorentz force in the y-direction	T_H	hot temperature [K]
G	gravitational acceleration, [m.s ⁻²]	U	dimensionless velocity in the x-direction
Gr	Grashof number ($= g\beta(T_H - T_C)H^3/\nu^2$)	u	velocity in the x-direction, [m.s ⁻¹]
H	height of the cavity, [m]	V	dimensionless vertical velocity.
Ha	Hartmann number ($= B_0 H \sqrt{\sigma/\rho\nu}$)	α	angle of orientation magnetic field Thermal diffusivity of the fluid
J_x	electric current in the x-direction, [A.m ⁻²]	γ	angle of inclination
J_y	electric current in the y-direction, [A.m ⁻²]	v	velocity in the y-direction, [m.s ⁻¹]
L	length of the enclosure, [m]	Φ	function
Nu	Nusselt average number	Γ	diffusivity term
P	pressure, [N.m ⁻²]		
Pr	Prandtl number ($= \nu/\alpha$)		

1. INTRODUCTION

Natural convection in closed enclosures has been extensively studied numerically and experimentally. The study of thermal convection in inclined enclosures is motivated by a desire to find out what effect slope would have on certain thermally driven flows which are found in many engineering applications.

These applications include: building systems containing multi-layered walls, double windows, and air gaps in unventilated spaces; energy systems such as solar collectors, storage devices, furnaces, heat exchangers, and nuclear reactors; material processing equipment such as melting and crystal growth reactors. Thermally driven flows are also found in large scale geophysical, astrophysical, and environmental phenomena.

Most of the research work that has been carried out in this area was focused on enclosures that were differentially heated in one direction (vertically or horizontally) with adiabatic side walls in the other direction. Rather little work has been carried out considering more complex thermal boundary conditions that are normally found in most of the aforementioned practical applications. In these applications, the imposed temperature gradient is neither horizontal nor vertical. Ostrach (1972), in his review on natural convection in enclosures, noted that configurations with more complex boundary conditions can be viewed as an exception among the works on this topic.

When the fluid is electrically conducting and exposed to a magnetic field the Lorentz force is also active and interacts with the buoyancy force in governing the flow and temperature fields. Employment of an external magnetic field has increasing applications in material manufacturing industry as a control mechanism since the Lorentz force suppresses the convection currents by reducing the velocities. Study and thorough understanding of the momentum and heat transfer in such a process is important for the better control and quality of the manufactured products. The study of Oreper and Szekely (1983) shows that the magnetic field suppresses the natural-convection currents and the magnetic field strength is one of the most important factors for crystal formation. Ozoe and Maruo (1987) numerically investigated the natural convection of a low Prandtl number fluid in the presence of a magnetic field and obtained correlations for the Nusselt number in terms of Rayleigh, Prandtl and Hartmann numbers. Garandet and al. (1992) proposed an analytical solution to the governing equations of magnetohydrodynamics to be used to model the effect of a transverse magnetic field on natural convection in a two-dimensional cavity. Rudraiah and al. (1995) numerically investigated the effect of a transverse magnetic field on natural-convection flow inside a rectangular enclosure with isothermal vertical walls and adiabatic horizontal walls and found out that a circulating flow is formed with a relatively weak magnetic field and that the convection is suppressed and the rate of convective heat transfer is decreased when the magnetic field strength increases. Alchaar and al.(1995) numerically investigated the natural convection in a shallow cavity heated from below in the presence of an inclined magnetic field and showed that the convection modes inside the cavity strongly depend on both the strength and orientation of the magnetic field and that horizontally applied magnetic field is the most effective in suppressing the convection currents. Al-Najem and al. (1998) used the power law control volume approach to determine the flow and temperature fields under a transverse magnetic field in a tilted square enclosure with isothermal vertical walls and adiabatic horizontal walls at Prandtl number of 0.71 and showed that the suppression effect of the magnetic field on convection currents and heat transfer is more significant for low inclination angles and high Grashof numbers. Mehmet Cem Ece and Elif

Büyük(2006)proposed laminar natural convection flows in the presence of a magnetic field in an inclined rectangular enclosure heated from the left vertical wall and cooled from the top wall while the other walls are kept adiabatic. The boundary conditions considered have a practical importance in cooled ceiling applications. The object of the study is to obtain numerical solutions for the velocity and temperature fields inside the enclosure and to determine the effects of the magnetic field strength and direction, the aspect ratio and the inclination of the enclosure on the transport phenomena.H. Wang and M.S. Hamed (2005) numerically investigated the combined effect of various bidirectional temperature gradients and angles of inclination on flow mode-transition and on hysteresis phenomenon (multi-steady solutions) in rectangular enclosures. Such combined effect, to the authors' knowledge, has not been investigated yet.S.K. Ghosh and I. Pop (2002) A note on a hydromagnetic flow in a slowly rotating system in the presence of an inclined magnetic field Magnetohydrodynamics. S.K. Ghosh and I. Pop (2006) An analytical approach to MHD plasma behavior of a rotating environment in the presence of an inclined magnetic field as compared to excitation frequency. S.K. Ghosh, O. Anwar Beg and M. Narahari (2013)a study of unsteadyrotating hydromagnetic free and forced convection in a channel subject to forced oscillation under an oblique magnetic field.M.N. Kherief and al (2012) obtained numerical solutions for the velocity and temperature fields inside the enclosure, to determine the effects of the magnetic field strength and direction, the inclination of the enclosure on the transport phenomena. The results show that the dynamic and temperature fields are strongly affected by variations of the magnetic field intensity and the angle of inclination. Numerical simulations have been carried out considering different combinations of Grashof and Hartmann numbers. Ghosh *and al.* (2010) proposed transient hydromagnetic flow in a rotating channel permeated by an inclined magnetic field with magnetic induction and Maxwell displacement current effects.The previous studies of the laminar natural-convection flows in the presence of a magnetic field inenclosures have dealt with thermal boundary conditions involving mostly isothermal vertical walls andadiabatic horizontal walls and a transverse magnetic field. The present study considers laminar naturalconvectionflows in the presence of a magnetic field ininclined rectangular enclosure heated from the left vertical wall and cooled from the top wall while the other walls are kept adiabatic. The boundary conditions considered have a practical importance in cooled ceiling applications. The object of the study is to obtain numerical solutions for the velocity and temperature fields inside the enclosure and to determine the effects of the magnetic field strength and direction, the aspect ratio and the inclination of the enclosure on the transport phenomena.

2. GEOMETRY AND MATHE- MATICAL MODEL

The geometry considered is a rectangular enclosure

having a length L and a width H , thus with an aspect ratio $A=L/H=4$, filled completely with a molten metal, the Prandtl number of which is $Pr=0.024$. Heated from one side and cooled from the adjacent side was considered, ($T_H > T_C$). The other walls are supposed to be adiabatic. The inclination of the cavity was also considered, with a varying angle γ . The flow is subjected to the action of an external uniform and constant magnetic field.

MHD flow, likely to develop in this enclosure, is governed by the equations of continuity, momentum, energy conservation, the Ohm's law and the conservation the electrical potential. The geometrical configuration is described in the Fig. 1.

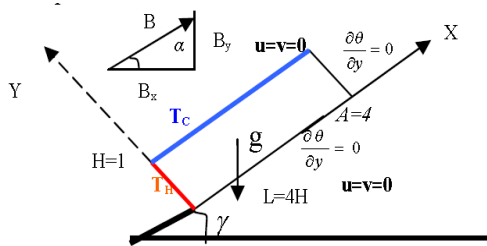


Fig. 1. The model problem.

The governing equations are obtained using the following assumptions:

1. Joule heating is negligible.
2. Viscous dissipation is negligible.
3. The induced magnetic field is negligible because $Re_m \ll 1$ (on the scale of the laboratory), Moreau (1991).
4. The liquid metal is not magnetized ($\mu_m=1$).
5. The liquid metal is incompressible and Newtonian.
6. The Boussinesq approximation holds.

The dimensionless governing equations for the conservation of mass, momentum, and energy, together with appropriate boundary conditions in the Cartesian coordinates system (x, y) , are written as follows:

$$\nabla \cdot \mathbf{V} = 0 \quad (1)$$

$$\frac{\partial \mathbf{V}}{\partial t} + (\mathbf{V} \cdot \nabla) \mathbf{V} = -\frac{1}{\rho} \nabla p + \nu \nabla^2 \mathbf{V} + g \beta (T - T_0) \mathbf{e}_y + \mathbf{F} \quad (2)$$

$$\frac{\partial T}{\partial t} + (\mathbf{V} \cdot \nabla) T = \alpha \nabla^2 T \quad (3)$$

Where, \mathbf{V} is the dimensional velocity vector, p is the dimensional pressure, T is the dimensional temperature, g is the gravitational acceleration, and ρ is the density, ν is the viscosity and α is the thermal diffusivity of the fluid, respectively.

The interaction between the magnetic field and convective flow involves an induced electric current \vec{j} :

$$\vec{j} = \sigma [-\vec{\nabla} \varphi + \vec{V} \times \vec{B}] \quad (4)$$

The divergence of Ohm's law $\vec{\nabla} \cdot \vec{j} = 0$ produces the equation of the electric potential:

$$\vec{\nabla}^2 \varphi = -\vec{\nabla} \cdot (\vec{V} \wedge \vec{e}_B) \quad (5)$$

Whereas those of \mathbf{F} have been obtained using the

equation:

$$\vec{F} = \vec{j} \times \vec{B} \quad (6)$$

By neglecting the induced magnetic field, the dissipation and Joule heating, and the Boussinesq approximation is valid; and using $H, \alpha/H, H^2/\alpha, \rho_0 (\alpha/H)^2, \alpha B_0$ and $(T_H - T_C)$ as typical scales for lengths, velocities, time, pressure, potential, and temperature, respectively, the dimensionless governing equations for the conservation of mass, momentum, and energy, together with appropriate boundary conditions in the Cartesian coordinates system (x, y) , are written as follows:

$$\frac{\partial U}{\partial X} + \frac{\partial V}{\partial Y} = 0 \quad (7)$$

$$\frac{\partial U}{\partial t} + U \frac{\partial U}{\partial X} + V \frac{\partial U}{\partial Y} = Gr \theta \sin \gamma - \frac{\partial P}{\partial X} + \left[\frac{\partial^2 U}{\partial X^2} + \frac{\partial^2 U}{\partial Y^2} \right] + F_{EMX} \quad (8)$$

$$\frac{\partial V}{\partial t} + U \frac{\partial V}{\partial X} + V \frac{\partial V}{\partial Y} = Gr \theta \cos \gamma - \frac{\partial P}{\partial Y} + \left[\frac{\partial^2 V}{\partial X^2} + \frac{\partial^2 V}{\partial Y^2} \right] + F_{EMY} \quad (9)$$

$$\frac{\partial \theta}{\partial t} + U \frac{\partial \theta}{\partial X} + V \frac{\partial \theta}{\partial Y} = \frac{1}{Pr} \left[\frac{\partial^2 \theta}{\partial X^2} + \frac{\partial^2 \theta}{\partial Y^2} \right] \quad (10)$$

Where: $Gr = g \beta (T_H - T_C) H^3 / \alpha^2$ is the Grashof number, $Ha = B_0 H \sqrt{\sigma / \rho \nu}$ the Hartmann number, and $Pr = \nu / \alpha$ the Prandtl number.

Where F_{EMX} and F_{EMY} represent respectively the dimensional forces of Lorentz following directions X and Y :

$$F_{EMX} = \sigma B_0^2 \left[(V \cos \alpha \sin \alpha - U \sin^2 \alpha) e_x \right] \quad (11)$$

$$F_{EMY} = \sigma B_0^2 \left[(U \sin \alpha \cos \alpha - V \cos^2 \alpha) e_y \right] \quad (12)$$

The initial conditions impose that the fluid is: At $t=0$, we have: $u = v = \theta = 0$.

At $t > 0$ the boundary conditions of the dimensionless quantities ($u, v, \text{ and } \theta$) are:

- At $X=0 \rightarrow \theta=1$ and $X=A \rightarrow \delta\theta/\delta y=0$.
- At $Y=1 \rightarrow \theta=0$ and $Y=0 \rightarrow \delta\theta/\delta y=0$.

3. NUMERICAL METHOD

The finite-volume method (1980), is used for the numerical resolution of the system of transport eq. (13):

$$\frac{\partial \varphi}{\partial t} + \frac{\partial (U_i \varphi)}{\partial X_i} = \frac{\partial}{\partial X_i} \left(\Gamma \varphi \frac{\partial \varphi}{\partial X_i} \right) + S_\varphi \quad (13)$$

The discretized form is:

$$A_P \varphi_P = A_E \varphi_E + A_W \varphi_W + A_N \varphi_N + A_S \varphi_S + b \quad (14)$$

The eq. (14) is solved using the SIMPLER algorithm (1980) the temporal derivative is

discretized using the implicit scheme. Concerning the spatial discretization, all the convective and the diffusive terms are discretized using the central differencing scheme.

Numerical scheme

The dimensionless governing equations were solved for stream function, vorticity and temperature using the *centered differences*. In this configuration, function $A(P)$ defined in the interfaces follows the following profile:

$$A(|P_i|) = 1 - 0.5|P_i| \quad (i = e, w, n, s) \quad (15)$$

This diagram is stable for $|P_i| \leq 2$, which ensures of the plus coefficients in the equation of discretization.

4. RESULTS AND DISCUSSION

a Code Validation in the Absence of a Magnetic Field

In the absence of a magnetic field, the momentum equation, eq. (2)-(4) are solved after setting $(F_x=F_y=0)$. The results are represented graphically in Figs. 3(a)-(d).

The flow structure is shown by the velocity vectors (Fig. 2(a)) and the velocity profiles (Figs. 2(a) and (b)). Fig. 2(a) shows that at the bottom of the cavity the flow is mainly longitudinal and is directed towards the hot wall (situated at $X = 0.0$) and at the top of the cavity the flow is directed towards the cold wall situated at $X = 4$. These boundary layers extend from the walls to the centre of the cavity, a behavior which is not common in ordinary fluids. From Figs. 2(a) and (b) one can notice that the U , and V profiles are linear throughout the core region extending from $(X = 0.25$ to $X = 0.75)$ and from $(Y = 0.25$ to $Y = 0.75)$. Comparison of Figs 2(a) and 2(b) reveals the expected behavior that the flow in the vertical direction is fastest because of the buoyancy-induced acceleration experienced by fluid particles transported in this direction.

A preliminary validation of the numerical method can be done, at this stage, via theoretical estimation of the magnitude of the maximum velocity, which is approximately 30 (Figs. 2(b) and (c)). One can, in effect, write, for large values of the Rayleigh number, that equilibrium exists between buoyancy forces and inertia forces, and has a value of 50. This explains the noticed distortion of the isotherms shown in Fig. 2(d).

The thermal structure of the flow is illustrated by the isotherms of Fig. 2(d) clearly shows the formation of thermal boundary layers along the vertical walls. Here also the temperature profiles in the core region extending from $X = 0.25$ to $X = 0.75$ are linear. As can be noticed from Fig. 2(d) plotted using a temperature increment $\Delta\theta = 0.05$ between two consecutive isotherms, the isotherms are denser on the lower part of the hot vertical wall and on the top part of the cold vertical wall. This indicates the presence of intense heat transfer across these parts

of the walls.

After that, we confronted our results with the results obtained by the references (1999) where the magnetic field is applied.

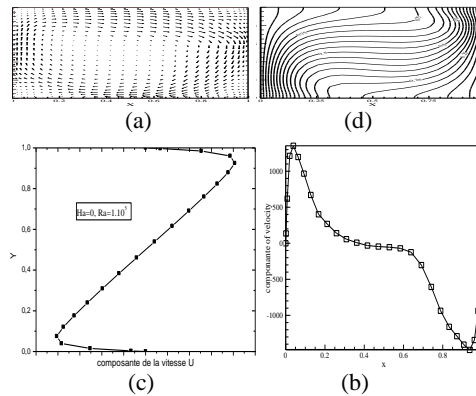
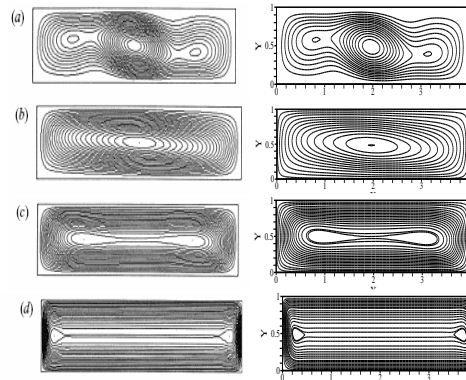


Fig. 2. (a) Velocity vector plot. (b) Distribution of vertical Velocity. (c) Distribution of horizontal Velocity. (d) Isotherms for $Ha=0$ and $Ra=10^5$.(1997)



Benhadid Results. Current results

Fig. 3. Validation of the results of the current functions obtained for various values of Hartmann with that from Ben Hadid : a- $Ha=0$; b- $Ha=5$; c- $Ha=10$; d- $Ha=100$, $Gr = 8 \times 10^2$, $Pr=0,01$, $A=4$.

In order to give a better insight into the physics behind the change in flow pattern, sketches of the current path corresponding to $Ha = 25$ and $Ha = 50$ are given, respectively, in Figs. 4(a) and (b).

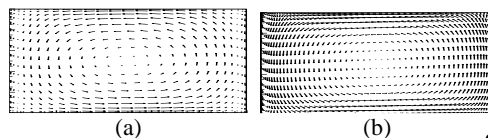


Fig. 4. (a) Current path for $Ha=25$. (b) Current path for $Ha=50$.

The Lorentz forces produced by the interaction between these currents and the applied vertical field are given, respectively, in Figs. 5(a) and (b). As can be noticed from Figs. 4, the flowing fluid generates under the action of the magnetic field, currents which are positive in the neighborhood of the top wall and negative in the neighborhood of the

bottom wall. This difference in sign is due to the different directions of the fluid in contact with the top and bottom walls. Because of this difference in sign, the Lorentz force acting on the top layers of the fluid is negative (i.e. a retarding force) and that acting on the bottom layers positive (i.e. also a retarding force since the fluid flows in the negative). When the value of Ha is increased, the magnitude of Lorentz forces increases (Fig. 5) and therefore reduces the magnitude of the velocity. This provokes the damping of the flow.

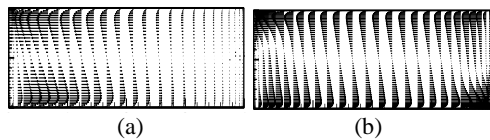


Fig. 5. (a) Component F_x of the Lorentz force for $Ra=800$ and $Ha=25$. (b) Component F_x of the Lorentz force for $Ra=800$ and $Ha=50$.

b Test and Choice the Grid

We go tested the effect of various kinds of grid to see the behavior of the Nusselt number average and the current function in the enclosure and this by fixing the following parameters: $Pr = 0.024$, $Gr = 5000$, $\alpha = 0$ and $Ha = 30$. With a dimensional step: $\Delta t=0,0001$.

Table 1 Tested the grid

Grid	$\overline{Nu} _{x=0}$	$\overline{Nu} _{x=A}$	Ψ_{max}	Ψ_{min}
82x32	0.2501304	0.2500866	1.794190	2.440E-07
98x42	0.2501372	0.2500819	1.790469	6.619E-07
112x42	0.2501345	0.2500816	1.789955	6.487E-07

The grid used for $Ha = 0$ was chosen after performing grid independency tests. The computed average Nusselt numbers for grids finer than 112x42 only differ hence the choice of this grid fig.6. Convergence of the numerical solution was obtained when the mass, momentum and energy residuals are below 10^{-4} .

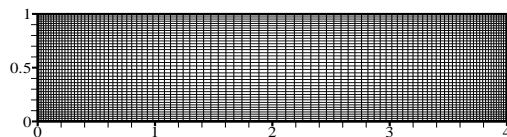


Fig. 6. Grid employed for the rectangular enclosure $A=4$.

c Discussion

Streamlines and isotherms for ($Ha = 0$) are presented herein Figs. 7–8 for various enclosure inclinations, When the enclosure is tilted 45° in the clockwise direction ($\gamma=-45^\circ$), the hot and cold walls form the upper left and right walls of the enclosure while the adiabatic walls constitute the lower walls. On the other hand, the hot and cold walls form the lower and upper left walls of the enclosure while the lower and upper right walls are adiabatic when

the enclosure is tilted 45° in the counterclockwise direction ($\gamma=45^\circ$). The buoyancy force which ascends the fluid particles heated near the hot acts parallel to the hot wall when the enclosure is not inclined but forces them toward and away from the hot wall when the enclosure is inclined in the clockwise and counterclockwise directions, respectively. Therefore, while the streamlines form a single eddy with clockwise rotation for $\gamma=0^\circ$ and -45° , a pair of counter-rotating eddies are formed for $\gamma=45^\circ$.

Circulation is weak due to relatively low Grashof number and the isotherms are spread almost radially between the hot and cold walls resembling heat transfer by pure conduction only.

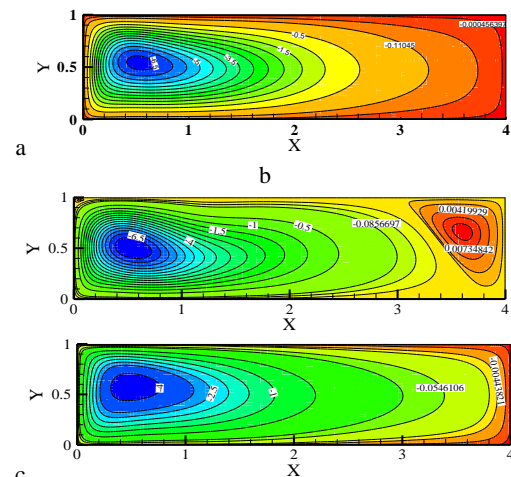


Fig. 7. Evolution of the current function for various orientation angle of the inclination. a) $\gamma=0^\circ$. b) $\gamma=45^\circ$. c) $\gamma=-45^\circ$. And $Ha=0$, $Gr=10000$, $\alpha=0^\circ$.

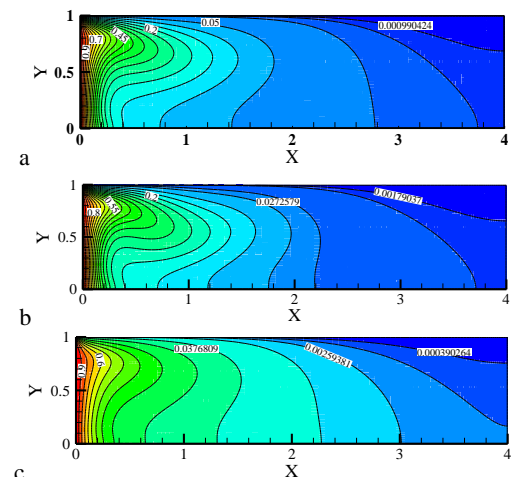


Fig. 8. Evolution of the Isotherm for various orientation angle of the inclination. a) $\gamma=0^\circ$. b) $\gamma=45^\circ$. c) $\gamma=-45^\circ$. And $Ha=0$, $Gr=10000$, $\alpha=0^\circ$.

Streamlines and isotherms in a tall rectangular enclosure with the presence of a strong magnetic field ($Ha = 100$) for various enclosure inclinations, magnetic field directions and Grashof numbers are

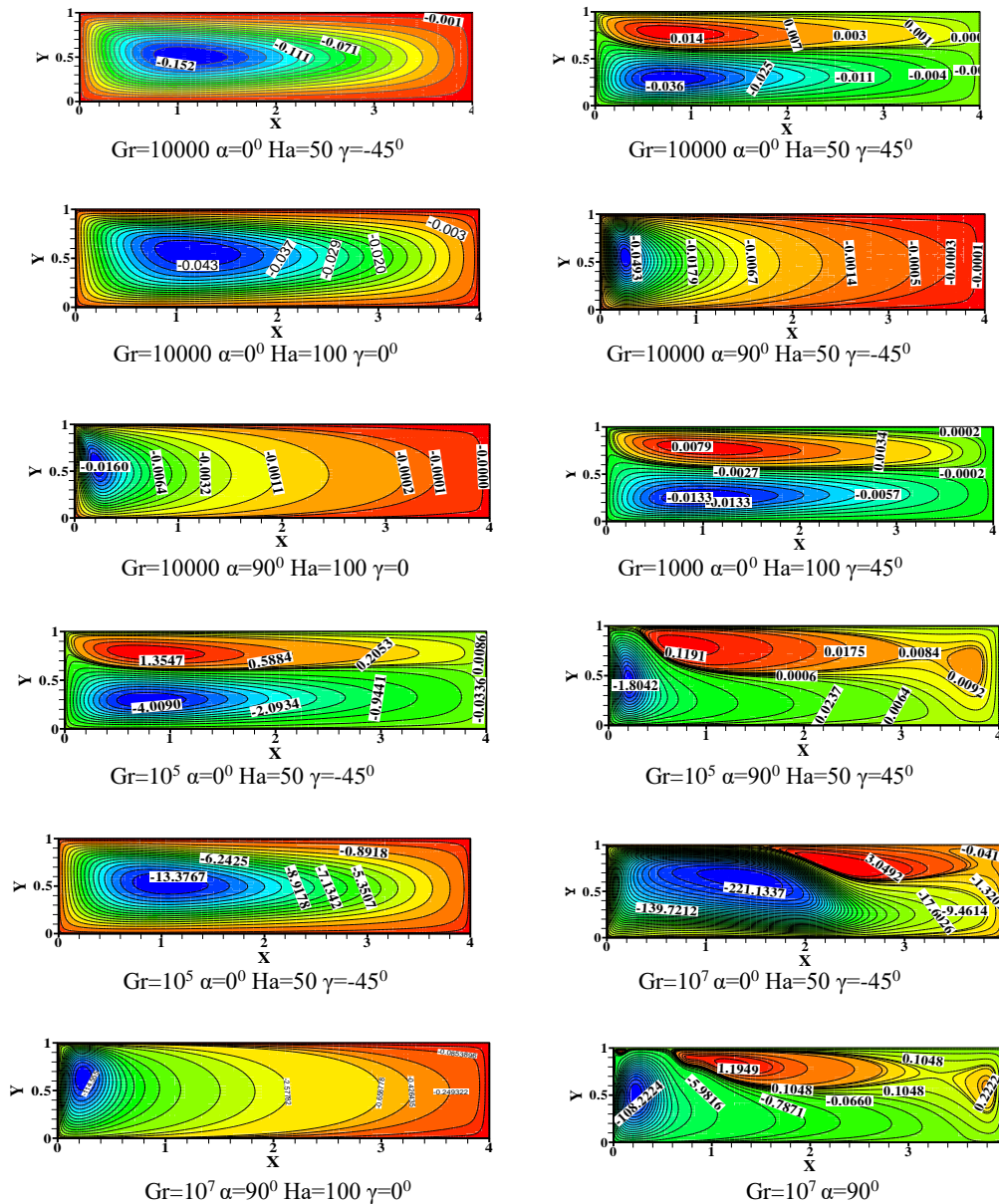


Fig. 9. Evolution of the current function for various Grashof numbers according to a Hartmann number, orientation angle of the magnetic field and the inclination angle.

shown in Figs. 9–10.

Figures show that the streamlines form a clockwise rotating eddy for cases of $\gamma=0^\circ$ and -45° . The strong magnetic field suppresses the circulation and vorticity. The center of the eddy is near the cold wall for magnetic field applied normal to the hot wall and near the hot wall for magnetic field applied normal to the cold wall due to the decelerating effect of the Lorentz force. The center of the eddy also shifts away from the magnetic flow direction when it is applied X-direction. The strong magnetic field suppresses both the circulation and vorticity. Circulation is increased by increasing Grashof number as it can be seen from the higher values of the streamlines. The isotherms are somewhat equally spaced or slightly deformed for $Gr = 10^4$ and they are bulged near the cold wall and squeezed near the lower hot wall as the Grashof number

increases up to 10^5 and 10^7 . This result is stronger when the magnetic field is applied normally to the cold wall ($\alpha=90^\circ$) and when the enclosure is tilted 45° in the clockwise direction ($\gamma=-45^\circ$) or not tilted ($\gamma=0^\circ$). The flow field displays a very complex pattern for the case of $\gamma=45^\circ$. There exist a pair of counter-rotating when the magnetic field is applied X-direction to the hot wall. The dividing extends diagonally from a point on the hot wall near the upper corner to a point on the upper right adiabatic wall near the lower corner. The lower eddy encloses two loops with a stagnation point between them for $Gr = 10^4$. When the magnetic field is applied Y-direction, the lower eddy is observed to extend to the cold wall and push the upper eddy toward the upper adiabatic wall.

The loops within the lower eddy are more visible in this case. As the magnetic field is further

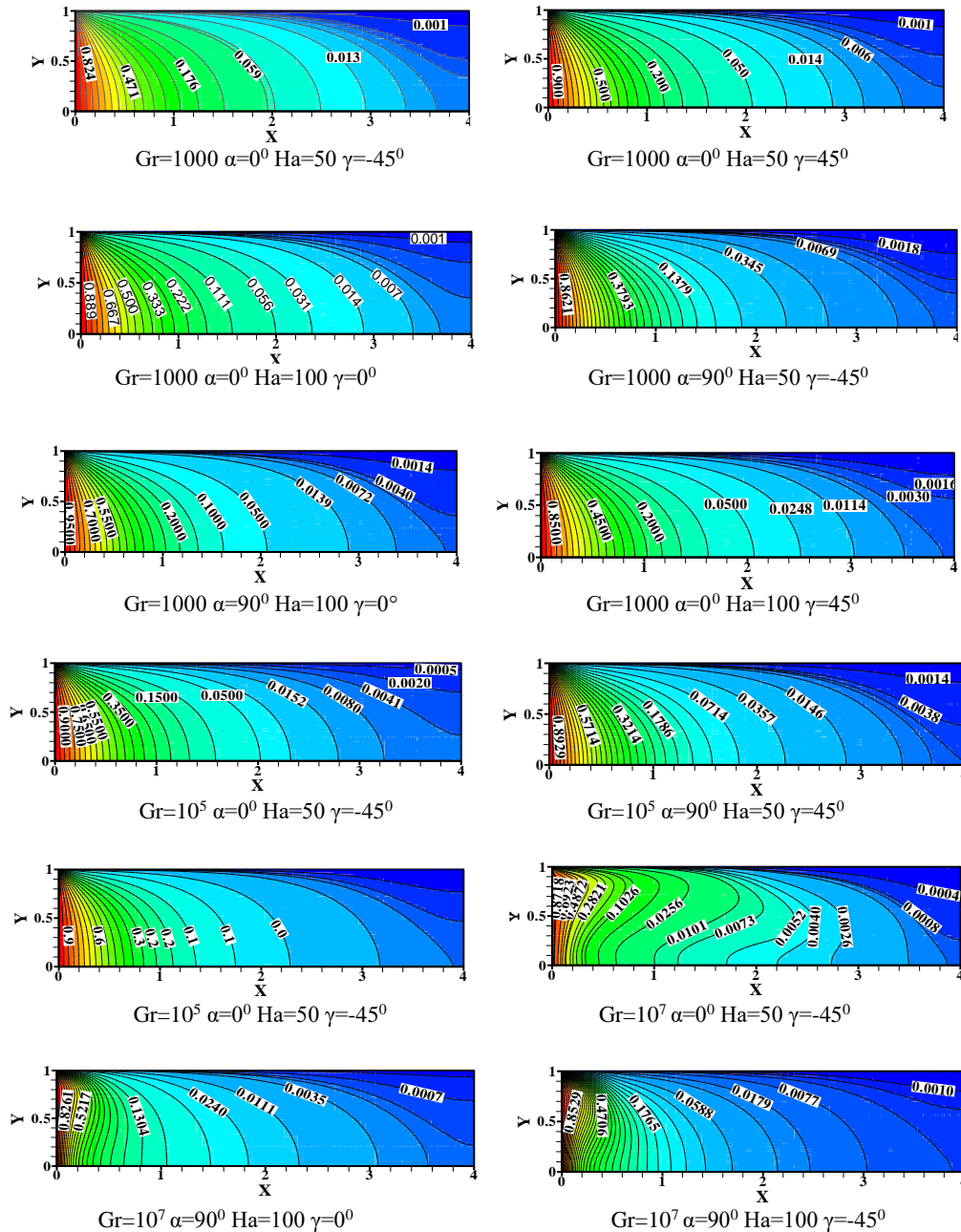


Fig. 10. Evolution of the Isotherm for various Grashof numbers according to a Hartmann number, orientation angle of the magnetic field and the inclination angle.

rotated counterclockwise and applied normal to the cold wall, the lower eddy grows along the hot wall with the loops disappearing and the dividing streamline is almost parallel to the hot wall. Circulation of eddies increases as the Grashof number increases and the loops within the lower eddy disappear when the magnetic field is applied X-direction to the hot wall. When the magnetic field is applied Y-direction, the upper eddy grows substantially and reaches the hot wall dividing the lower eddy into multiple eddies.

However, when the magnetic field is applied X-direction to the cold wall, a pair of counter-rotating eddies are formed with the dividing streamline almost parallel to the hot wall. The isotherms are

almost equally spaced between the hot and cold walls for $Gr = 10^4$ but the increased circulation and the formation of multiple eddies cause a kinky behavior in the isotherms for $Gr = 10^5$ and $Gr = 10^7$.

We notice that for a small number of Gr , the flow generates very weak velocity gradients, when the Gr number increases; the flow induced by the increasing buoyancy forces becomes animated. Significant velocity gradients are then localized near the walls, resulting in the production of multiple eddies or vortices. This is well illustrated in Figs. 11-a, b and c.

Concerning the horizontal normalized velocity profiles, they are shown in Figs. 11 of the X-

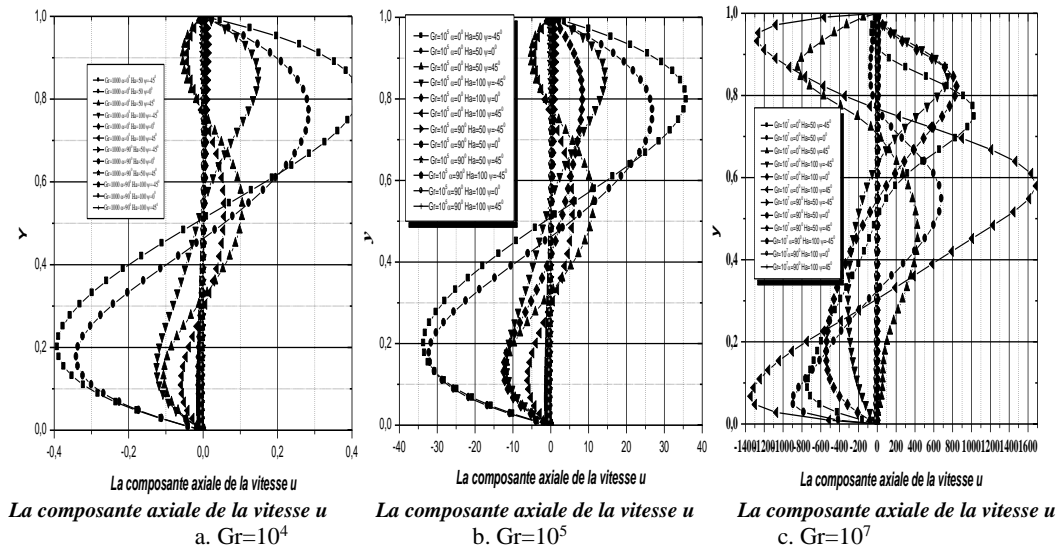


Fig. 11. Evolution speed horizontal component in the enclosure center for various Grashof numbers according to a Hartmann number, orientation angle magnetic field and the inclination angle.

Table 2 Variation of the average Nusselt number

γ	Gr	Nu (Ha=0)	Nu (Ha=100)	
			$\alpha=0^\circ$	$\alpha=90^\circ$
0°	10^3	2.065639	1.995967	1.997511
	10^4	2.649331	1.993139	1.996799
	10^5	3.889977	1.952511	2.436661
	10^7	15.763160	4.637601	3.062145
-45°	10^3	2.088343	1.696850	1.700009
	10^4	2.701963	1.695311	1.798000
	10^5	3.971976	1.795707	2.017178
	10^7	16.763160	5.001252	5.235416
45°	10^3	1.588343	1.797200	1.786333
	10^4	2.301963	1.782006	1.756609
	10^5	3.071976	1.802794	1.846667
	10^7	10.763160	3.095472	3.999420

direction magnetic field and Y-direction magnetic field.

It is clear from the results that as Ha are increased; the velocity components tend to diminish. In fact, for $Ha=100$, their values are practically equal to zero in the major part of the cavity except near the end walls. It is clear that the use of a magnetic field can strongly decrease the flow intensity, but cannot completely inhibit fluid motion.

The enclosure slope has a strong effect on the flow and the heat transfer behavior. A single cell is obtained; it appears to be completely stable, symmetrical and fills all the enclosure, the effect of inclination on the velocity diminishes in the presence of the magnetic field.

Average Nusselt numbers are listed in Table 2. Average Nusselt number increases naturally with Grashof number and it is substantially reduced by the magnetic field. The magnetic field applied Y-direction to the hot wall is more effective reducing

the convection and therefore the heat transfer for enclosure and the magnetic field applied Y-direction to the cold wall is more effective reducing the convection for shallow enclosures. The average Nusselt number is slightly reduced by the counterclockwise inclination in the enclosure. The effect of inclination on the average Nusselt number diminishes in the presence of the magnetic field.

5. CONCLUSIONS

The present study considers laminar natural-convection flow in the presence of a magnetic field in an inclined rectangular enclosure heated from the left vertical wall and cooled from the top wall while the other walls are kept adiabatic. The flow characteristics and the convection heat transfer inside the tilted enclosure, depend strongly upon the strength and direction of the magnetic field and the inclination of the enclosure. Circulation and convection become stronger with increasing Grashof numbers but they are significantly

suppressed by the presence of a strong magnetic field. As a result, formation of multiple eddies of counterclockwise inclination greatly influences the temperature field.

The local Nusselt number increases considerably with Grashof number since the circulation becomes stronger.

The magnetic field significantly reduces the local Nusselt number by suppressing the convection currents.

REFERENCES

- Alchaar, S., P. Vasseur and E. Bilgen (1995). The effect of a magnetic field on natural convection in a shallow cavity heated from below. *Chem. Eng. Commun.* 134, 195–209.
- Al-Najem, N. M., K. M. Khanafer and M. M. El-Refae (1998). Numerical study of laminar natural convection in tilted enclosure with transverse magnetic field. *Int. J. Numer. Methods Heat Fluid Flow*, 8, 651–672.
- Benhadid, H. and D. Henry (1997). Numerical study of convection in the horizontal Bridgman conuration under the action of a constant magnetic field, Part2, Three-dimensional flow *Journal of Fluid Mechanics* 333, 57-83.
- Bessaih R., M. Kadja and Ph. Marty (1999). Effect of wall electrical conductivity and magnetic field orientation on liquid metal flow in geometry similar to the horizontal Bridgman configuration for crystal growth, *International Journal of Heat and Mass Transfer* 42, 4345-4362.
- Garandet, J. P., T. Alboussiere and R. Moreau (1992). Buoyancy drive convection in a rectangular enclosure with a transverse magnetic field. *Int. J. Heat Mass Transfer* 35, 741–748.
- Ghosh, S. K. (2010). Transient hydromagnetic flow in a rotating channel permeated by an inclined magnetic field with magnetic induction and Maxwell displacement current effects. *Zeitschrift fur angewandte Mathematik und Physik, ZAMP* 61(1), 147–169.
- Ghosh, S. K. and I. Pop (2002). A note on a hydromagnetic flow in a slowly rotating system in the presence of an inclined magnetic field. *Magneto hydrodynamics* 38(4), 377 – 384.
- Ghosh, S. K. and I. Pop (2006). An analytical approach to MHD plasma behavior of a rotating environment in the presence of an inclined magnetic field as compared to excitation frequency. *Int. J. of Applied Mechanics and Engineering* 11(4), 845-856.
- Ghosh, S. K., A. O. Beg and M. Narahari (2013). A study of unsteady rotating hydromagnetic free and forced convection in a channel subject to forced oscillation under an oblique magnetic field. *Journal of Applied Fluid Mechanics* 6(2), 213 – 227.
- Kherief, M. N., K. Talbi and F. Berrahil (2012). Effects of Inclination and Magnetic Field on Natural Convection Flow Induced by a Vertical Temperature. *Journal of Applied Fluid Mechanics* 5(1), 113-1 20.
- Mehmet, C. E. and B. Elif (2006). Natural-convection flow under a magnetic field in an inclined rectangular enclosure heated and cooled on adjacent walls. *Fluid Dynamics Research* 38, 564–590.
- Moreau, R. (1991). *Magneto hydrodynamics*. Kluwer Academic Publishers, 36-39.
- Oreper, G. M. and J. Szekely (1983). The effect of an externally imposed magnetic field on buoyancy driven flow in a rectangular cavity. *J. Cryst. Growth* 64, 505–515.
- Ostrach, S. (1972). Natural convection in enclosure. In: Hartnett, J.P., Irvine, T.F. (Eds.), *Advances in Heat Transfer*, 8, 161-227.
- Ozoe, H. and M. Maruo (1987). Magnetic and gravitational natural convection of melted silicon-two dimensional numerical computations for the rate of heat transfer. *JSME* 30, 774–784.
- Patankar, S.V. (1980). *Numerical Heat Transfer and Fluid Flow*, Hemisphere: Washinton DC.
- Rudraiah, N., R. M. Barron, M. Venkatachalappa and C. K. Subbaraya (1995). Effect of a magnetic field on free convection in a rectangular enclosure. *Int. J. Eng. Sci.* 33, 1075–1084.
- Wang, H., M. S. Hamed (2005). Flow mode-transition of natural convection in inclined rectangular enclosures subjected to bidirectional temperature gradients, *International journal of Thermal Sciences*.